UDK 66.017:669.018.9:620.178.3
Original scientific article/Izvirni znanstveni članek

ISSN 1580-2949
MTAEC9, 49(1)99(2015)

MICROMECHANICAL MODEL OF THE SUBSTITUENTS OF A UNIDIRECTIONAL FIBER-REINFORCED COMPOSITE AND ITS RESPONSE TO THE TENSILE CYCLIC LOADING

MIKROMEHANSKI MODEL NADOMESTKOV KOMPOZITOV, OJAČANIH Z ENOSMERNIMI VLAKNI, IN NJIHOV ODGOVOR NA CIKLIČNO NATEZNO OBREMENJEVANJE

Tomáš Kroupa[1], Hana Srbová[2], Robert Zemčík[1]

[1]University of West Bohemia in Pilsen, NTIS – New Technologies for the Information Society, Univerzitní 22, 306 14, Plzeň, Czech Republic
[2]University of West Bohemia in Pilsen, Department of Mechanics, Univerzitní 22, 306 14 Plzeň, Czech Republic
kroupa@kme.zcu.cz

Prejem rokopisa – received: 2013-11-08; sprejem za objavo – accepted for publication: 2014-02-13

A micromechanical model respecting the behavior of a long-fiber unidirectional composite subjected to the cyclic tensile loading was proposed. The so-called unit cell representing the structure of the composite material was created using the finite-element-analysis software. Material models of the fibers and matrix proposed in this work are based on the non-linear elastic and elasto-plastic behavior of real materials. The material and geometric parameters of the model are found by minimizing the difference between the numerical and experimental results.

Keywords: unidirectional fiber composite, cyclic tensile test, micromodel, material parameters, non-linear, elasto-plastic

Predlagan je mikromehanski model, ki obravnava vedenje kompozita z dolgimi enosmernimi vlakni pri cikličnemu nateznemu obremenjevanju. Osnovna celica, ki pomeni zgradbo kompozita, je bila izdelana s programsko opremo za analizo končnih elementov. Predlagani model materiala vlaken in osnove temelji na nelinearnem elasto-plastičnem vedenju realnih materialov. Material in geometrijski parametri modela so dobljeni z zmanjševanjem razlike med numeričnimi in eksperimentalnimi rezultati.

Ključne besede: kompozit z enosmernimi vlakni, ciklični natezni preizkus, mikromodel, parametri materiala, nelinearno, elasto-plastično

1 INTRODUCTION

Due to advantages, such as stiffness-to-weight and strength-to-weight ratios, carbon-fiber-reinforced composites are widely used for load-carrying structures in various kinds of industries such as aerospace, automotive, etc.

The behavior of composite materials can be modeled on the micro-, meso- and macro-scale levels. The micromechanical approach gives the most detailed information about the constituents. The constituents and the resulting composite exhibit, in general, a significantly non-linear response. In this work, the material models of the constituents include non-linear elastic and elasto-plastic effects. The goal is to capture the response of a unidirectional composite to the cyclic loading.

2 EXPERIMENT

In this work carbon-epoxy unidirectional continuous-fiber-composite-coupons were subjected to the tensile cyclic loading. Rectangular specimens (coupons) were cut with a water jet from a composite plate made of eight equally oriented layers, the so-called prepregs, HexPly 913C with fiber Tenax HTS 5631. With respect to the loading direction five specimens were tested for each of the following fiber orientations: 10°, 20°, 30°, 40°, 50°, 60°, 70°, 80° and 90° (**Figure 1**). Only two specimens were successfully tested for the fiber orientation of 0°. All the specimens were loaded in tension

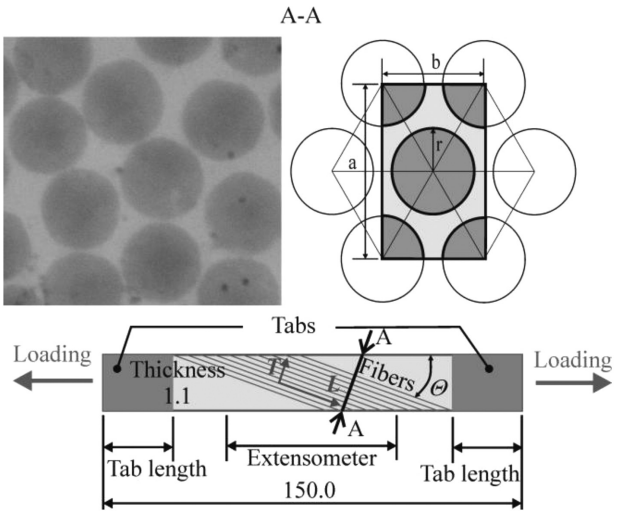

Figure 1: Geometry of the coupons (mm), real and idealized parts of the composite cross-section with a unit cell

Slika 1: Geometrija vzorcev (mm), realen in idealiziran del prereza kompozita z osnovno celico

with the constantly increasing cycles up to failure. The test control parameter was the applied load.

The force-displacement dependencies obtained from the experiment were measured on the coupons with the glass-textile (0°) or aluminum tabs (10°, 20°, 30°, 40°, 50°, 60°) bonded with epoxy high-strength and tough adhesive Spabond 345. In the cases of the specimens with the fiber orientations of 70°, 80° and 90° a non-bonded emery cloth was used as the interface between the grip and the coupon. The tab configuration summarized in **Table 1** produced the required gage-section tensile failure (**Figure 2**).[1]

Table 1: Experiment configuration
Tabela 1: Konfiguracija eksperimenta

Fiber orientation (°)	Tab material	Tab length (mm)	Extensometer length (mm)
0	glass textile	60.0	10.0
10, 20, 30, 40, 50, 60	aluminum	25.0	60.0
70, 80, 90	emery cloth	25.0	60.0

2.1 Micromodel (finite-element model)

A three-dimensional idealized micromechanical model of the composite material was proposed in the form of a unit cell representing the periodical array of the composite. The unit cell consists of two parts, the part of the matrix and the part of the fibers. The fibers and the matrix are perfectly bonded.

A perfect honeycomb distribution of the fibers is assumed and the ratio of *r*:*a*:*b* (**Figure 1**) is given by the fiber volume ratio V_f. The finite-strain theory was used.

The global coordinate system *xyz* is given by the loading direction *x* and the direction perpendicular to the composite surface *z*. The local coordinate system 123 is defined by the unit-cell edges, where the axis direction 1 corresponds to the fiber direction, direction 3 is identical to the axis direction *z* and 2 is perpendicular to axes 1 and 3 (**Figure 3**).

Assuming a uniaxial stress across the whole specimen, the behavior of the material can be simulated by loading the unit cell with a normal stress:

$$\sigma_x = \frac{F}{A} \tag{1}$$

where *F* is the external force and *A* is the cross-section of the specimen.

The effect of the loading force is transformed to the local coordinate system using the transformation:

$$\begin{bmatrix} \sigma_1 \\ \sigma_2 \\ \tau_{12} \end{bmatrix} = \begin{bmatrix} \cos^2\theta & \sin^2\theta & 2\sin\theta\cos\theta \\ \sin^2\theta & \cos^2\theta & -2\sin\theta\cos\theta \\ -\sin\theta\cos\theta & \sin\theta\cos\theta & \cos^2\theta - \sin^2\theta \end{bmatrix} \cdot \begin{bmatrix} \sigma_x \\ 0 \\ 0 \end{bmatrix} \tag{2}$$

where θ is the angle of rotation between the local and global coordinate systems.[2]

The results from the finite-element analysis (strains) are transformed back to the global coordinate system using the transformation:

$$\begin{bmatrix} \varepsilon_x \\ \varepsilon_y \\ \gamma_{xy} \end{bmatrix} = \begin{bmatrix} \cos^2\theta & \sin^2\theta & -\sin\theta\cos\theta \\ \sin^2\theta & \cos^2\theta & \sin\theta\cos\theta \\ 2\sin\theta\cos\theta & -2\sin\theta\cos\theta & \cos^2\theta - \sin^2\theta \end{bmatrix} \cdot \begin{bmatrix} \varepsilon_1 \\ \varepsilon_2 \\ \gamma_{12} \end{bmatrix} \tag{3}$$

Periodical boundary conditions were applied to ensure that there was no separation or overlap between the neighboring unit cells after the deformation.[2,3]

The micromodel was built in Abaqus/CAE (Complete Abaqus Environment), consisting of eight-node brick elements. The finite-element analysis was solved as a quasistatic process using the Abaqus/standard solver. The loading respected the experimentally obtained envelope; however, only four cycles were prescribed to reduce the computational time.

2.2 Material model of the fibers

The fibers were modeled as a transversely isotropic, elastic material, respecting the non-linear behavior in the axis direction. The nonlinearity is ensured with the form of the stress-strain relationships:

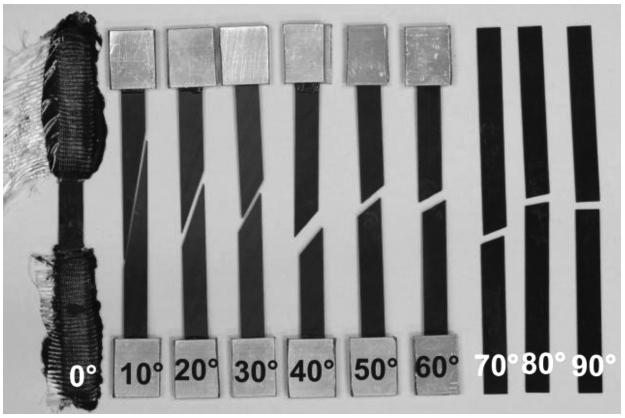

Figure 2: Cracked specimens. Final crack direction is parallel to the fibers in the directions of 10°–90° and perpendicular for the direction of 0°.
Slika 2: Vzorci z razpoko. Končna smer razpoke je vzporedna z vlakni pri smereh 10°–90° in pravokotna pri smeri 0°.

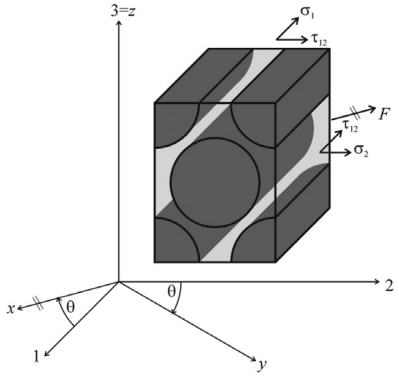

Figure 3: Rotated coordinate systems and loading of the unit cell
Slika 3: Zavrteni koordinatni sistemi in obremenitev osnovne celice

$$\begin{aligned}
\sigma_{11} &= C_{11}(1+\tfrac{1}{2}\xi\varepsilon_{11})\varepsilon_{11} + C_{12}(\varepsilon_{22}+\varepsilon_{33}) \\
\sigma_{22} &= C_{12}\varepsilon_{11} + C_{22}\varepsilon_{22} + C_{23}\varepsilon_{23} \\
\sigma_{33} &= C_{12}\varepsilon_{11} + C_{23}\varepsilon_{22} + C_{22}\varepsilon_{33} \\
\tau_{12} &= G_{12}\gamma_{12} \\
\tau_{13} &= G_{12}\gamma_{13} \\
\tau_{23} &= G_{23}\gamma_{23}
\end{aligned} \tag{4}$$

where ξ is the coefficient describing the measure of nonlinearity with the growing strain ε_{11} in the fiber direction, while ε_{22} and ε_{33} are the strains in the directions transverse to the fibers. G_{12} and G_{13} are the shear moduli in planes 12 and 13, respectively. The remaining elastic constants are:

$$\begin{aligned}
C_{11} &= \frac{E_1(1-\nu_{23}^2)}{1-\nu_{12}\nu_{21}-\nu_{23}^2-2\nu_{21}^2\nu_{23}} \\
C_{12} &= \frac{E_1\nu_{21}(1+\nu_{23})}{1-\nu_{12}\nu_{21}-\nu_{23}^2-2\nu_{21}^2\nu_{23}} \\
C_{13} &= C_{12} \\
C_{22} &= \frac{E_2(1-\nu_{31}\nu_{12})}{1-\nu_{12}\nu_{21}-\nu_{23}^2-2\nu_{21}^2\nu_{23}} \\
C_{23} &= \frac{E_2(\nu_{23}+\nu_{21}\nu_{12})}{1-\nu_{12}\nu_{21}-\nu_{23}^2-2\nu_{21}^2\nu_{23}} \\
C_{33} &= C_{22}
\end{aligned} \tag{5}$$

where E_1 is the Young's modulus in the fiber direction, E_2 is the Young's modulus in the direction transverse to the fibers and ν_{12}, ν_{21} and ν_{23} are Poisson's ratios.[4]

2.3 Material model of the matrix

The matrix was modeled as an isotropic, elasto-plastic material. The elastic parameters were Young's modulus E_m and Poisson's ratio ν_m. Von Mises plasticity was used with the isotropic-hardening and work-hardening functions proposed in the form of:

$$\sigma^y = \sigma_0^y + \beta(\bar{\varepsilon}_p)^\alpha \tag{6}$$

where σ^y is the yield stress, $\bar{\varepsilon}_p$ is the equivalent plastic strain, σ_0^y is the initial yield stress, and β and α are the shape parameters.

2.4 Identification process

The experimental results from the tensile cyclic tests were processed using the Python programming language. For each set of experiments belonging to the fiber direction θ, the arithmetic mean of displacement values at the maximum point of each cycle, was found. By connecting these averaged points with lines, the envelope curve was obtained. Tangent k of a particular cycle was determined by approximating the peak points with a linear function:

$$F = k\Delta l + q \tag{7}$$

individually for each experiment (**Figure 4**).

During the process of material-parameter optimization, the residuum describing the difference between the experimentally obtained envelope curve consisting of N points and the numerical force-displacement data for the cyclic tensile test:

$$r = \sum_{\theta}\sum_{i=1}^{N}\left(\frac{\Delta l^{\exp}(\theta, F_i) - \Delta l^{\text{num}}(\theta, F_i)}{\Delta l_N^{\exp}(\theta)}\right)^2 \tag{8}$$

is minimized.

3 RESULTS

Material parameters were found for V_f = 0.55 and r:a:b = 1:1.28:2.22 (**Tables 2** and **3**). Moreover, the inaccuracy of the cutting orientation of the samples from the plate was determined to be $\Delta\theta$ = 1.7°.

The work-hardening function is shown in **Figure 5**. Note that the force-displacement dependencies resulting from the numerical analysis are in good agreement with the dependencies obtained experimentally (**Figures 6** and **7**). However, there is not sufficient agreement between the cycle tangents (**Figure 8**).

Table 2: Material parameters of fibers
Tabela 2: Parametri materiala vlaken

Parameter	Units	Value
E_1	(GPa)	155.77
ξ	(-)	14.44
E_2	(GPa)	16.41
ν_{12}	(-)	0.30
ν_{23}	(-)	0.40
G_{12}	(GPa)	50.35

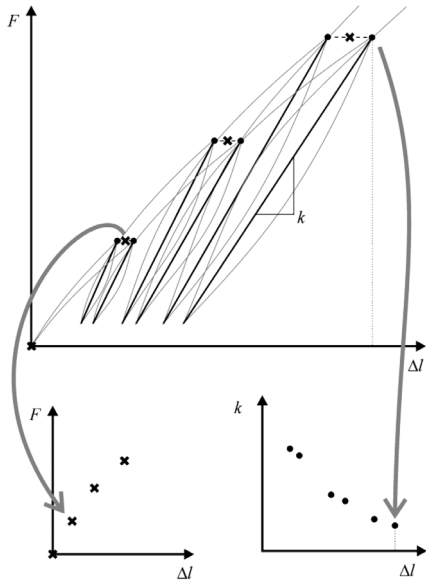

Figure 4: Principle of processing the data experimentally obtained from multiple experiments into envelope curve $F(\Delta l)$ and cycle tangents $k(\Delta l)$
Slika 4: Način pridobitve eksperimentalnih podatkov iz večkratnih preizkusov v skupno krivuljo $F(\Delta l)$ in tangento ciklov $k(\Delta l)$

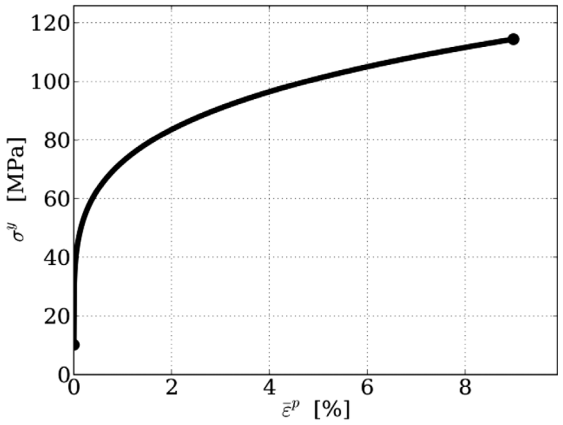

Figure 5: Matrix work-hardening function
Slika 5: Funkcija utrjevanja osnove

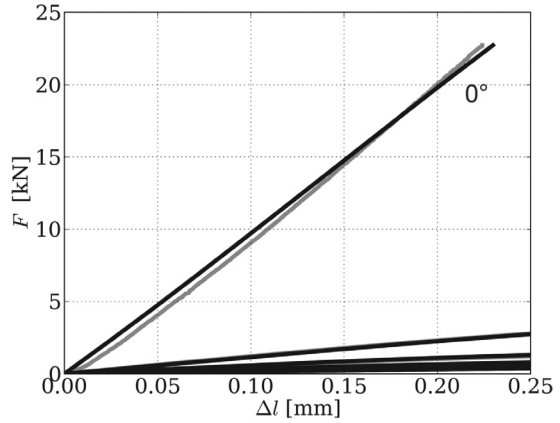

Figure 6: Force-displacement diagrams for the 0° specimen (black – determined, gray – experiments)
Slika 6: Diagrami sila – raztezek pri vzorcu 0° (črno – določeno, sivo – eksperimenti)

Table 3: Matrix-material parameters
Tabela 3: Parametri osnovnega materiala

Parameter	Units	Value
E_m	(GPa)	3.97
ν_m	(–)	0.40
σ_0^y	(MPa)	10.14
α	(–)	0.23
β	(MPa)	182.71

4 CONCLUSION

Finite-element analyses of the cyclic tensile tests were performed on unidirectional composite specimens with various fiber orientations. Material parameters of the orthotropic non-linear elastic material of the fibers and of the non-linear elasto-plastic material of the matrix were determined and good agreement with the experiments was achieved.

In future work a degradation of the matrix will be included into the material model in order to achieve better agreement between the determined and experimentally obtained cycle tangents.

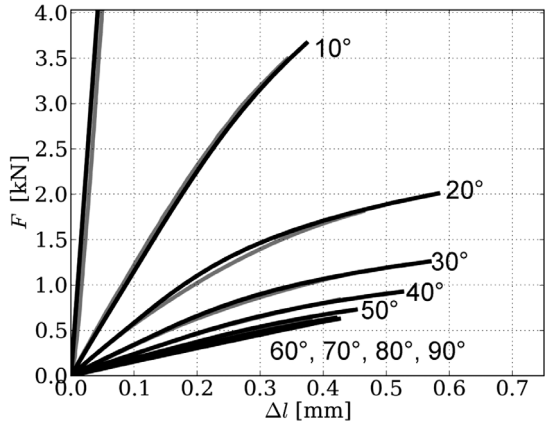

Figure 7: Force-displacement diagrams for 10° to 90° specimens (black – determined, gray – experiments)
Slika 7: Diagrami sila – raztezek pri vzorcih od 10° do 90° (črno – določeno, sivo – eksperimenti)

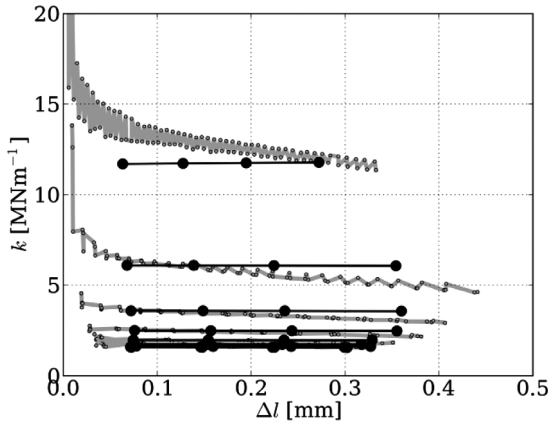

Figure 8: Tangents of the force-displacement cycles (black – determined, gray – experiments)
Slika 8: Tangente ciklov sila – raztezek (črno –določeno, sivo – eksperimenti)

Acknowledgement

The work was supported by projects SGS-2013-036 and European Regional Development Fund (ERDF), project "NTIS - New Technologies for the Information Society", European Centre of Excellence, CZ.1.05/1.1.00/02.0090.

5 REFERENCES

[1] ASTM Standard D 3039/D 3039M - 08, 2008, Standard Test Method for Tensile Properties of Polymer Matrix Composite Materials, ASTM International, West Conshohocken, PA 19428-2959, 2003, www.astm.org

[2] H. Srbová, T. Kroupa, R. Zemčík, Identification of the Material Parameters of a Unidirectional Fiber Composite Using a Micromodel, Mater. Tehnol., 46 (**2012**) 5, 431–434

[3] S. W. Tsai, P. D. Shah, Strength & Life of Composites, Department of Aeronautics & Astronautics, Stanford University, 2008

[4] V. Laš, Mechanics of Composite Materials, University of Bohemia, Plzeň, 2004 (in Czech)